

Low-Temperature Magnetic Susceptibility and Heat Capacity of GdAsO_4

J. H. Colwell, B. W. Mangum, and D. D. Thornton*†

National Bureau of Standards, Washington, D. C. 20234

(Received 3 February 1971)

We report measurements obtained in zero applied magnetic field of the magnetic susceptibility and heat capacity of GdAsO_4 in the temperature range 0.3–20 K. This material is antiferromagnetic below 1.262 K. A detailed comparison of the experimental results is made with those reported for the isomorphous compound GdVO_4 . The entropy and energy of GdAsO_4 above and below the Néel temperature are in close agreement with the predictions of the Heisenberg model suggesting that the interactions are not only isotropic, but predominantly with the nearest neighbors as well. The magnetic measurements, on the other hand, indicate considerable anisotropy such that GdAsO_4 does not undergo a spin-flop transition. Attempts to explain this discrepancy are given. We have derived a value of the exchange-interaction constant $J/k \approx -0.04$ K, assuming a coordination number of 4 where J is defined by the Hamiltonian

$$\mathcal{H} = -2 \sum_{i < j} J_{ij} \vec{S}_i \cdot \vec{S}_j - g\mu_B \sum_i \vec{H}_0 \cdot \vec{S}_i.$$

In this communication the results of magnetic susceptibility and heat capacity measurements on single crystals of GdAsO_4 are reported. These results are of particular interest because of comparisons that can be made with the isomorphous compound GdVO_4 which has been reported recently by Cashion *et al.*¹ Both of these materials order antiferromagnetically in the liquid-helium range because of interactions between the Gd^{3+} ions whose ground state is $^8S_{7/2}$. The crystals have the zircon structure² which has tetragonal symmetry. The space group is D_{4h}^{19} ($I4/amd$), and the unit-cell dimensions are $a_0 = 0.71326$ nm, $c_0 = 0.63578$ nm for GdAsO_4 and $a_0 = 0.7211$ nm, $c_0 = 0.6350$ nm for GdVO_4 . There are four gadolinium ions per unit cell, all magnetically equivalent, which lie on a slightly distorted diamond lattice. There are four magnetic nearest neighbors surrounding each Gd^{3+} ion. Since the only apparent difference between these two materials is the atoms at the centers of the oxygen tetrahedra which form the anions, we have an opportunity to compare the magnetic interactions of the Gd^{3+} ions on nearly identical lattices. However, we find that a very marked difference exists in that the transition temperature T_N of the arsenate is only one-half that of the vanadate, indicating that the interactions between Gd^{3+} ions are considerably different. Beyond that, the two materials have generally similar behavior, but close examination turns up many differences which are not readily explained.

The GdAsO_4 crystals were grown by J. N. Lee of Johns Hopkins University using the $\text{Pb}_2\text{P}_2\text{O}_7$ flux method described by Feigelson.³ The crystals were not chemically analyzed but were of excellent optical quality. The individual crystals were typically

$0.5 \times 0.5 \times 3$ mm³ in size.

The heat capacity was determined using a sample consisting of about ten single crystals and weighing 0.042 g. Measurements were made between 0.3 and 3 K using the incremental heating method in an apparatus described elsewhere.^{4,5} The sample was attached with varnish to a copper sample mounting. The sample mounting, thermometer, and heater which made up the calorimetric addenda has a heat capacity approximately equivalent to 3 g of copper. The uncertainty in the accuracy of the measurements was less than 1% over most of the temperature range but increased to about 2% at 3 K because of reduced thermometer sensitivity. The addenda heat capacity is less than 1% of the total in the region of the transition and is only 3% at 0.3 K. The addenda contribution becomes appreciable at higher temperatures; it is 15% at 2 K and reaches 36% at 3 K. Consequently, the uncertainty in the sample heat capacity is less than 1% up to about 2 K but may be as large as 5% at 3 K.

The results, shown in Fig. 1, represent only the magnetic heat capacity, since the lattice contribution¹ is negligible in the temperature range of the measurements. One can calculate that the hyperfine contribution is also negligible. The sharp peak indicating the onset of antiferromagnetic order in GdAsO_4 is at 1.262 ± 0.002 K.⁶ For comparison, the results reported for GdVO_4 are shown as the solid curve in Fig. 1 with the temperature scale normalized so that T_N is the same as that for GdAsO_4 . As can be seen, the heat capacities of the two materials are very similar. The maximum values of C/R observed are 6.1 and 6.3 for the arsenate and vanadate, respectively. The behavior of GdAsO_4 close to T_N is portrayed in Fig. 2, where

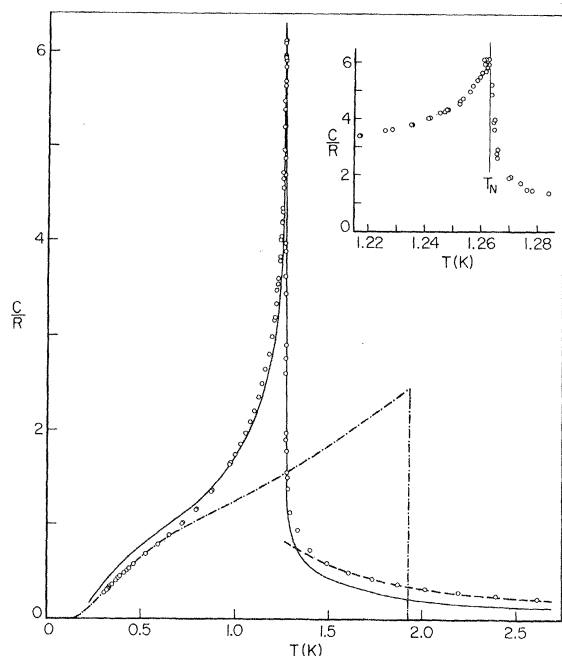


FIG. 1. Heat capacity of GdAsO_4 compared with that of GdVO_4 and with that calculated by using the molecular-field theory. Open circles represent the data for GdAsO_4 . The solid curve represents the data for GdVO_4 (Ref. 1) normalized to $T_N = 1.262$ K, that of GdAsO_4 . The dot-dashed curve is calculated for a spin- $\frac{7}{2}$ system using the molecular-field approximation with $T_N = 1.92$ K. The dashed line is the curve of $C/R = 1.28/T^2$. The inset shows the critical region on an expanded scale.

the heat capacity is plotted versus $t = |T - T_N|/T_N$ on semilog and log-log plots. We have used $T_N = 1.262$ K, the Néel temperature determined by the maximum in the heat capacity and by the maximum in $\partial(\chi T)/\partial T$. In the range $t = 10^{-1} - 10^{-3}$, the heat capacity for $T < T_N$ appears to have a logarithmic dependence, whereas for $T > T_N$, the data appear to have a power-law dependence. In Fig. 2 the solid lines through the data are given by

$$C/R = -0.875 \ln t + 0.45, \quad T < T_N$$

and

$$C/R = 0.327 t^{-0.36}, \quad T > T_N.$$

A quite similar dependence was found with GdVO_4 ¹ where, for the same ranges of t , the heat capacity could be represented by

$$C/R = -0.722 \ln t + 0.74, \quad T < T_N$$

and

$$C/R = 0.32 t^{-0.30}, \quad T > T_N.$$

The other interesting feature of the heat capacity of GdAsO_4 , as well as of GdVO_4 , is the rounded shoulder at low temperatures. This behavior is

typical of that observed in other antiferromagnetic materials having high spin values, e.g., MnF_2 ,⁷ $\text{MnCl}_2 \cdot 4\text{H}_2\text{O}$,⁸ and GdAlO_3 .⁹ Following the example of Stout and Catalano,⁷ we have calculated the heat capacity for a spin- $\frac{7}{2}$ system using the molecular-field approach outlined by Van Vleck¹⁰ and have plotted the result as the dot-dashed curve in Fig. 1. The calculated heat capacity was fitted to the data in the region of the shoulder by variation of T_N , recognizing that T_N is considerably overestimated by this model, particularly for the case of small coordination numbers. With $T_N = 1.92 \pm 0.05$ K, the theory accurately ($\pm 1\%$) represents the data from the lowest measurement at 0.3 K to approximately 0.63 K, i.e., one-half the experimental T_N . The ratio of $T_N(\text{molecular field})$ to $T_N(\text{expt})$ is 1.52. The molecular-field theory gives a similarly good

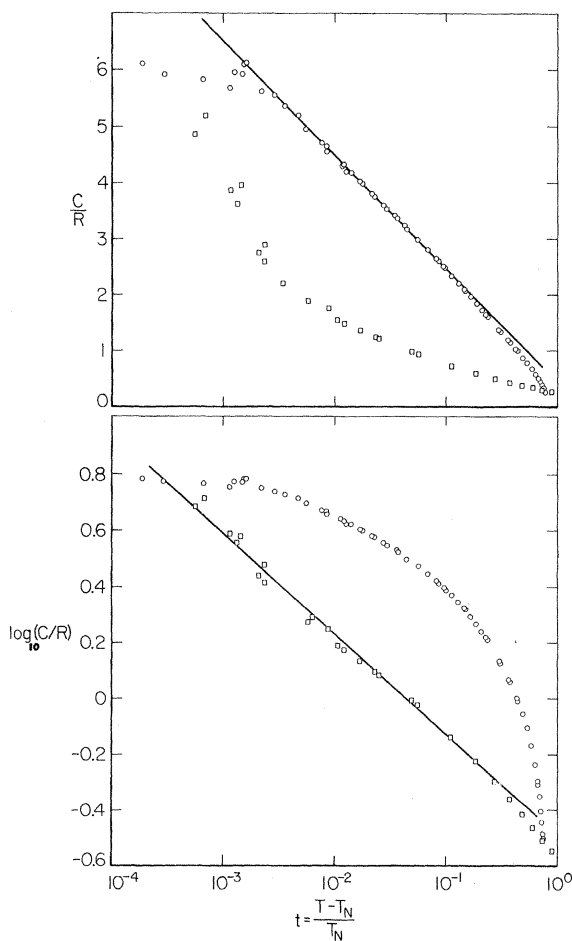


FIG. 2. Plot of the heat capacity and its logarithm vs the logarithm of $t \equiv |T - T_N|/T_N$. The upper graph shows the apparent logarithmic dependence of the heat capacity for $T < T_N$. The straight line is given by $C/R = -0.875 \ln t + 0.45$. The lower graph shows the apparent power-law dependence of the data for $T > T_N$. The straight line is given by $C/R = 0.327 t^{-0.36}$.

fit to the GdVO_4 data up to ~ 1.0 K with $T_N = 3.35 \pm 0.10$ K, but here the ratio of T_N (molecular field) to T_N (expt) is only 1.34.

The dashed curve in Fig. 1 for $T > T_N$ is given by the expression $C/R = 1.28/T^2$ which is taken to be the high-temperature limiting behavior of the magnetic heat capacity. One can see in Fig. 1 that this term is proportionately much larger than that in the vanadate. It may also seem somewhat surprising that the $1/T^2$ behavior in GdAsO_4 persists so close to T_N . Essam and Sykes¹¹ have shown, however, that Ising interactions of ions of spin- $\frac{1}{2}$ on a diamond lattice give a heat capacity which behaves in much the same way. In addition, Domb and Sykes¹² have shown that the high-temperature heat capacity of a Heisenberg system with large spin has nearly the same temperature dependence as that for an Ising system of spin- $\frac{1}{2}$. This suggests, then, a small "effective coordination number" in GdAsO_4 . It should be noted that in GdVO_4 the $1/T^2$ dependence does not persist nearly as close to T_N .

The susceptibility of single crystals of GdAsO_4 was measured from 0.3 to 20 K, both parallel and perpendicular to the tetragonal axis, by the ac mutual-inductance method. The results are shown in Fig. 3, where the circles and squares represent the parallel and perpendicular susceptibilities, respectively. In the high-temperature region ($T \gg T_N$) the magnetic susceptibility should follow a Curie-Weiss law,

$$\chi = \frac{Ng^2\mu_B^2 S(S+1)}{3k(T+\theta)},$$

where one would expect that the g tensor would be isotropic with $g=2$, since Gd^{3+} is an S -state ion. Since the samples were approximately the shape of long prolate ellipsoids, the data were corrected for

demagnetizing effects to correspond to that of a spherically shaped sample. In this form the susceptibility was, in fact, isotropic and obeyed the Curie-Weiss law for temperatures above 9 K. The value of the Weiss constant obtained is $\theta = -0.65 \pm 0.4$ K which implies ferromagnetic interactions. Below 9 K the parallel and perpendicular susceptibilities diverge from each other and from the Curie-Weiss behavior. At about 1.4 K the parallel component passes through a maximum, and then decreases rapidly toward zero as the temperature is lowered. The perpendicular component also exhibits a maximum slightly below 1.3 K, but becomes essentially constant from 1 K to the lowest temperature. This behavior is typical of a two-sublattice uniaxial antiferromagnet. In Fig. 4 we show the parallel component of the susceptibility in the transition region. On the expanded scale the maximum in the slope at T_N can be seen clearly.

The entropy and energy changes associated with the magnetic ordering have been derived from the heat capacity. The molecular-field model is assumed to represent the heat capacity at low temperatures, and the $1/T^2$ behavior is assumed at high temperatures. The experimental entropy obtained in this way is $S/R = 2.08_6$ which agrees with the expected value of $S/R = \ln 8 = 2.079$ to well within the 1% uncertainty quoted for the heat-capacity data. This result is not particularly dependent on the precise nature of the extrapolations used for the heat capacity beyond the range of the data, since these contributions to S/R as calculated amount to only 0.070 below 0.3 K and 0.102 above 2.5 K. The determination of the total magnetic energy is more dependent on the high-temperature extrapolation where 21% of the energy change occurs above 2.5 K.

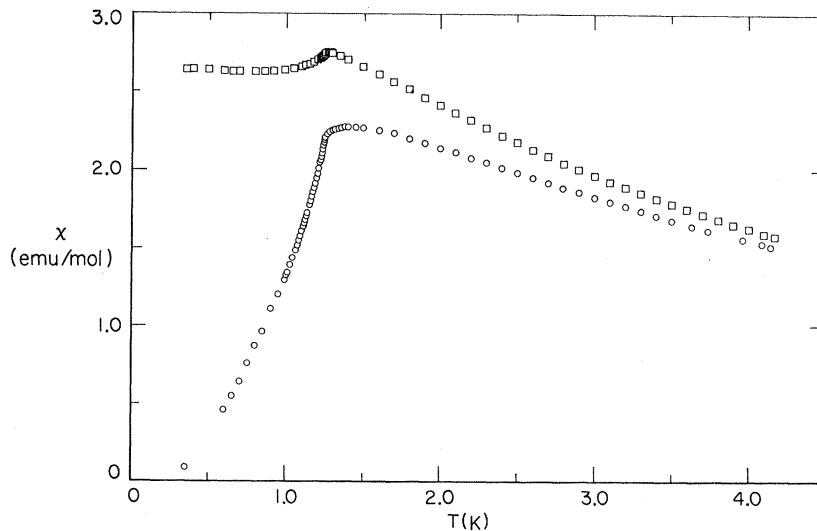


FIG. 3. Molar magnetic susceptibility of a single crystal of GdAsO_4 which has been corrected for demagnetizing effects to give the value corresponding to a spherical specimen. Open circles represent the data obtained with the measuring field parallel to the tetragonal axis. The squares represent the data obtained with the measuring field perpendicular to that axis.

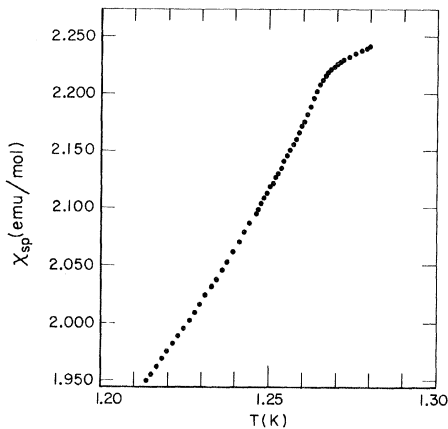


FIG. 4. Parallel susceptibility of a single crystal of GdAsO_4 in the region of the Néel point on an expanded scale. The susceptibility has been corrected for demagnetizing effects to give the value corresponding to a spherical specimen.

In Table I the entropy and reduced energy, as distributed above and below T_N , are presented for GdAsO_4 and GdVO_4 . The experimental values are compared with theoretical values that are based on model calculations where the interactions considered are either Heisenberg or Ising exchange interactions between nearest-neighbor ions only. Precise values of these critical entropies and energies have been calculated for various lattice structures and spin values.¹³ Unfortunately, they have not been determined for the diamond lattice (coordination number $q=4$) or for spin $S=\frac{7}{2}$ for either type of interaction. As a result, we are forced to use estimated values determined from the collection of values for other lattices and spin values. The values given in Table I for the Heisenberg and Ising models were obtained by correlating the known critical values as functions of $1/q$ and $1/S$. These estimates are believed to be accurate to within 10%.

Table I shows very clearly that there is a distinct difference between the magnetic behavior of GdAsO_4 and that of GdVO_4 . The critical values of the arsenate agree well with those of the $q=4$ Heisenberg model, while the values for the vanadate are close to those of either the Ising model or the fcc Heisenberg model. If one compares the experimental values with the predictions for the diamond lattice, $q=4$, the implication is that the interactions in the vanadate are more anisotropic than those in the arsenate, whereas the opposite would be the more reasonable expectation. This may be seen if one considers the three identifiable contributions to the magnetic energy: the exchange and dipolar interactions between ions, and the single-ion crystal-field energy which arises from the interactions of the ions with the lattice. In the case

of GdVO_4 , Cashion *et al.*¹ have assigned values to each of these contributions. The dipolar contribution was obtained by a direct computation of the dipole sums for the antiferromagnetically ordered state assuming a two-sublattice model. The crystal field contribution was established using the difference between the anisotropy field, determined from magnetization measurements, and the calculated dipolar anisotropy field. The exchange energy was taken as the difference between the total energy and the sum of the crystal field and dipolar energies. For GdAsO_4 the dipolar energy is essentially identical to that of GdVO_4 . The crystal field contribution has not been determined, but we assume it to be the same as that in the vanadate, which is reasonable in view of the fact that they have essentially the same unit-cell dimensions. The exchange contribution is again taken as the difference between the sum of these terms and the total energy. In Table II the relative amounts of these different contributions to the total energies of GdAsO_4 and GdVO_4 are compared. The exchange coupling in both materials is between S-state ions and, therefore, can be described by isotropic Heisenberg interactions. With the dipole and crystal field effects being equal in the two materials, one would expect the vanadate, with its larger exchange interaction, to agree more closely with the Heisenberg model, but the heat capacities indicate otherwise.

The divergence of the susceptibilities, parallel and perpendicular to the symmetry axis, which occurs above the Néel temperature must also arise from anisotropy effects. This divergence is greater in the arsenate than it is in the vanadate. In all of the gadolinium compounds reported in the literature which become antiferromagnetic, the susceptibility perpendicular to the symmetry axis is larger than that parallel to the symmetry axis above T_N . In GdAsO_4 this effect is particularly pronounced. This feature is difficult to explain since both the crystal field and dipolar anisotropies would act to

TABLE I. Critical values for GdAsO_4 and GdVO_4 compared with estimates for Heisenberg and Ising models with $S=\frac{7}{2}$.

	$\frac{S_N}{R}$	$\frac{S_\infty - S_N}{R}$	$\frac{E_N - E_0}{RT_N}$	$\frac{E_\infty - E_N}{RT_N}$	$\frac{E_\infty - E_0}{RT_N}$
Heisenberg model					
Diamond lattice	1.6	0.5	1.0	0.8	1.8 ^a
GdAsO_4	1.64 ₀	0.44 ₆	1.08 ₄	0.85 ₁	1.93 ₅
GdVO_4	1.768	0.272	1.121	0.433	1.554
Ising model					
Diamond lattice	1.85	0.23	1.1	0.4	1.5
Heisenberg model ^b					
fcc lattice	1.77	0.31	1.03	0.46	1.49

^aThis value has also been given by C. Domb, see Ref. 1

^bThese values were given in Ref. 1.

TABLE II. Contributions to the total magnetic energies of GdAsO₄ and GdVO₄.

Contribution	GdAsO ₄		GdVO ₄	
	$\Delta E/R$ (K)	% of total	$\Delta E/R$ (K)	% of total
Total	2.45 ₄	100	3.88	100
Dipolar	0.35	14	0.35	9
Crystalline field	0.20	8	0.20	5
Exchange	1.91 ₃	78	3.34	86

reduce the perpendicular component above T_N , assuming the crystal field has the same sign as that reported for GdVO₄.¹ Also, one must rule out anisotropy in the g factor, since the susceptibility is isotropic in the liquid-hydrogen region. This leaves, then, the unattractive alternative of anisotropic exchange in a system consisting of S -state ions. At least in the case of GdVO₄, even this possibility is unlikely and, if present, it must be relatively unimportant since in that material there is a clear case of spin flop.¹ Preliminary measurements of the magnetization, at temperatures far below the Néel point, indicate that a simple case of spin flop does not occur in GdAsO₄,¹⁴ whereas GdVO₄ undergoes a classic textbook-type spin flop.^{1,15} These arguments indicate that GdAsO₄ is considerably more anisotropic than GdVO₄, whereas the opposite viewpoint was reached in considering the thermodynamic critical values which are usually quoted to indicate that a material can be represented by either an Ising or Heisenberg model.

To check the consistency of the experimental results, we have derived values of the interaction constant J/k using various theoretical expressions dependent on this parameter. This has been carried out in much the same manner as that used by Cashion *et al.* for GdVO₄¹ (and GdAlO₃)⁹; there, a value of $J/k = -0.063$ K was obtained. The exchange-interaction constant is defined by

$$\mathfrak{H} = -2 \sum_{i < j} J_{ij} \vec{S}_i \cdot \vec{S}_j,$$

where the summation is assumed to be over nearest neighbors only. The crystalline electric field is assumed to have the simple axial form

$$\mathfrak{H} = D[S_z^2 - \frac{1}{3}S(S+1)],$$

where we have used $D = -0.03$ K as found for GdVO₄.¹

In GdAsO₄ the dipolar interactions are an appreciable part of the total interaction. The dipolar term can be explicitly separated in calculating the total energy and the high-temperature heat capacity (if one neglects cross terms which are assumed to be small), but in the other expressions it has not been considered. As a result we have listed in Table III values of J/k which include the dipolar

contribution, so that, in a sense, they represent the total magnetic interaction between the ions. In the two cases where the dipolar contributions can be separated, the "pure" exchange constants are listed. With the exception of the value derived from the Weiss constant, there is good agreement between the interaction constants, particularly when one considers the different measurements and temperature regions involved. The agreement may be fortuitous to some extent, because the different parameters will be affected differently by the dipolar interactions. The two cases listed in Table III,

TABLE III. Values of the interaction constant derived by various methods. Values are given with the dipolar contribution included and, where possible, with it separated.

Method	J/k (K)	
	Dipolar interactions included	Dipolar interactions separated
Total energy ^a	-0.044	-0.038
Parallel susceptibility at T_N ^b	-0.043	
Weiss constant ^c	+0.015	
Perpendicular susceptibility at $T = 0$ ^d	-0.038	
Rushbrooke and Wood prediction of T_N ^e	-0.046	
High-temperature heat capacity ^f	-0.044	-0.032
Low-temperature heat capacity ^g	-0.046	
Parallel susceptibility at $T \ll T_N$ ^h	-0.041	

^aTotal energy as derived from the heat capacity is given by $E_\infty - E_0 = Nq |J| S^2 [1 + (0.6/qS)] + \frac{1}{3} N |D| S(2S-1) + \frac{1}{2} Ng \mu_B^2 SH_d$, where the extra factor in the exchange term accounts for the uncertainty in the antiferromagnetic ground state (Ref. 16), and H_d is the dipolar interaction field in the ordered state.

^bMolecular-field theory gives the parallel susceptibility at the Néel point as $\chi_{||}(T_N) = Ng^2 \mu_B^2 / 4qJ$ which Lines (Ref. 17) has shown to be independent of crystal field anisotropy effects.

^cThe Weiss constant is related to J/k by the molecular-field formula $qJ/k = 3\theta/2S(S+1)$.

^dSusceptibility perpendicular to the symmetry axis at $T = 0$ as used in a method described by Lines (Refs. 17 and 18).

^eRushbrooke and Wood (Ref. 19) used series-expansion techniques to derive the expression

$$kT_N/J = \frac{5}{96} (q-1) [11S(S+1) - 1] [1 + 2/3qS(S+1)].$$

^fLimiting high-temperature heat capacity is given by

$$\frac{CT^2}{R} = \frac{2qJ^2S^2(S+1)^2}{3k^2} + \frac{D^2S(S+1)(2S-1)(2S+3)}{45k^2} + 379 [g^2 \mu_B^2 J(J+1)/k]^2.$$

The numerical coefficient of the dipolar contribution, the last term, contains structural factors as derived by Van Vleck (Ref. 20).

^gMolecular-field model fitted to the heat-capacity data as shown in Fig. 1.

^hParallel susceptibility from spin-wave theory (Ref. 21).

where the dipolar dependence has been determined, probably represent extreme examples, since the states represented are those of complete order at $T=0$ and of high-temperature short-range order. Therefore, it is not unreasonable to assign a value of $J/k = -0.035$ K to the exchange interaction excluding dipolar contributions with an estimated uncertainty of about 10%. The value of J/k obtained from the Weiss constant (as well as the Weiss constant itself) is, of course, in poor agreement with the other results. This, however, may be a result of a relatively strong ferromagnetic interaction with more distant neighbors which does not compete with the antiferromagnetic interaction. In fact, both the second- and fourth-nearest-neighbor dipolar interactions are of this kind.

The main difficulty in rationalizing the differences between GdAsO_4 and GdVO_4 is probably associated with the comparison of the critical values with those predicted by the Heisenberg and Ising models which consider near-neighbor interactions only. The presence of exchange interactions other than those between nearest neighbors can account for some of the observed differences. The experimental results require that the net interaction in the vanadate be approximately twice that of the arsenate. This could occur by having higher-neighbor interactions present in the vanadate which enhance the near-neighbor interactions or by having such interactions in the arsenate act in opposition to the near-neighbor interaction. Dalton and Wood²² have calculated the effects that next-nearest-neighbor interactions have on the critical behavior. An interaction which contributes to the resultant long-range order will increase T_N , while one that opposes the long-range order will result in T_N being decreased. A consequence of this is that the portions of the energy and entropy changes which occur above T_N are decreased where the interactions reinforce each other, and increased where they are in opposition. Both of these effects are probably required to account for the experimentally observed critical values. In GdAsO_4 , the crystal field and dipolar anisotropies would be expected to have some influence on the critical values, but none is apparent. This could result from these anisotropy effects having little influence on the critical values, or possibly there are higher-neighbor exchange interactions which cancel their influence. In GdVO_4 anisotropy effects must be smaller than in GdAsO_4 ; thus, to explain the observed critical values, one must conclude that there are higher-neighbor interactions which enhance the long-range

ordering. Calculations of the effects of higher-neighbor interactions have not been carried out for the diamond lattice, so quantitative comparisons with theory cannot be made. However, results for other lattices indicate that shifts in the critical values would be particularly pronounced with the diamond lattice because of the small number of nearest neighbors. In Table I we have included the critical values for the Heisenberg model for a face-centered cubic lattice to indicate how changes in coordination number affect the critical values. The close agreement of the GdVO_4 results with this model has already been pointed out by Cashion *et al.*¹ It is not unreasonable to make the comparison, since if higher-neighbor interactions are comparable in magnitude with the near-neighbor interactions, the result is an effective increase in coordination number. The smaller ratio $T_N(\text{molecular field})/T_N(\text{expt})$ and the deviation of the heat capacity from the $1/T^2$ behavior at temperatures considerably above T_N can also be taken as evidence that the effective coordination number in GdVO_4 is greater than that in GdAsO_4 . A probable reason for the pronounced difference in the interactions between these two materials is the fact that the V^{5+} ion has an empty $3d$ shell, whereas the As^{5+} ion has a filled $3d$ shell.

In conclusion, it appears that the magnetic data indicate that GdAsO_4 is considerably more anisotropic than GdVO_4 . Comparisons of the thermodynamic critical values derived from the heat-capacity data with values calculated for Heisenberg and Ising models with near-neighbor interactions suggest that the opposite is the case. The apparent discrepancy in the thermodynamic values is probably due, at least in part, to the failure to include higher-neighbor interactions in the model calculations. The values for GdAsO_4 agree with those for a Heisenberg model with nearest-neighbor interactions only and show no apparent effect from dipolar or crystalline field anisotropies. A Heisenberg model which includes strong interactions from more than just near-neighbor ions is required to explain the GdVO_4 results. Our combined results indicate, then, that comparisons of experimental critical values predicted by model calculations can be misleading when used as a means of determining the type of interactions in a system.

We would like to express our gratitude to J. N. Lee and Professor H. W. Moos for providing us with the crystals used in this study and to Dr. A. H. Cooke for providing us with his heat-capacity data on GdVO_4 .

*National Research Council—National Bureau of Standards Postdoctoral Research Associate 1968–70.

†Present address: Department of Physics, Syracuse University, Syracuse, N. Y. 13210

- ¹J. D. Cashion, A. H. Cooke, L. A. Hoel, D. M. Martin, and M. R. Wells, Proc. Colloq. Intern. CNRS Eléments Terres Rares 180, 417 (1970).
- ²R. W. G. Wyckoff, *Crystal Structures*, 2nd. ed. (Interscience, New York, 1965), Chap. VIII.
- ³R. S. Feigelson, J. Am. Ceram. Soc. 47, 257 (1964).
- ⁴J. C. Wright, H. W. Moos, J. H. Colwell, B. W. Mangum, and D. D. Thornton, Phys. Rev. B 3, 843 (1971).
- ⁵J. H. Colwell, Rev. Sci. Instr. 40, 1182 (1969).
- ⁶This temperature is based on the NBS Provisional Temperature Scale 2-20 (1965); H. Plumb and G. Catalano, Metrologia 2, 127 (1966).
- ⁷J. W. Stout and E. Catalano, J. Chem. Phys. 23, 2013 (1955).
- ⁸A. R. Miedema, R. F. Wielinga, and W. J. Huiskamp, Physica 31, 835 (1965).
- ⁹J. D. Cashion, A. H. Cooke, T. L. Thorp, and M. R. Wells, Proc. Roy. Soc. (London) A318, 473 (1970).
- ¹⁰J. H. Van Vleck, J. Chem. Phys. 9, 85 (1941).
- ¹¹J. W. Essam and M. F. Sykes, Physica 29, 378 (1963).
- ¹²C. Domb and M. K. Sykes, Phys. Rev. 128, 168 (1962).
- ¹³See, for example, C. Domb and A. R. Miedema, in *Progress in Low-Temperature Physics*, edited by C. J. Gorter (North-Holland, Amsterdam, 1964), Vol. IV, Chap. 4; M. E. Fisher, Rept. Progr. Phys. 30, 615 (1967).
- ¹⁴B. W. Mangum and D. D. Thornton, in *Proceedings of the Twelfth International Conference on Low Temperature Physics, Kyoto, Japan, 1970* (Keigaku Publishing, Tokyo, Japan, 1971).
- ¹⁵B. W. Mangum and D. D. Thornton (unpublished).
- ¹⁶F. Keffer, in *Handbuch der Physik*, edited by S. Flügge (Springer, Berlin, 1966), Vol. 18, Part 2, p. 1.
- ¹⁷M. E. Lines, Phys. Rev. 135, A1336 (1964).
- ¹⁸M. E. Lines, Phys. Rev. 156, 543 (1967).
- ¹⁹G. S. Rushbrooke and P. J. Wood, J. Mol. Phys. 1, 257 (1958); 6, 409 (1963).
- ²⁰J. H. Van Vleck, J. Chem. Phys. 5, 320 (1937).
- ²¹R. Kubo, Phys. Rev. 87, 568 (1952).
- ²²N. W. Dalton and D. W. Wood, Phys. Rev. 138, A779 (1965); 159, 384 (1967); J. Math. Phys. 10, 1271 (1969).

Spin Reorientation in ErFeO₃ Single Crystals Observed by Neutron Diffraction

H. Pinto, G. Shachar, and H. Shaked

Department of Physics, Nuclear Research Centre-Negev, P. O. B. 9001, Beer-Sheva, Israel
and

S. Shtrikman

Department of Electronics, The Weizmann Institute of Science, Rehovot, Israel

(Received 9 December 1970)

Neutron diffraction from a single crystal of ErFeO₃ confirms that the spin reorientation at about 95°K does not occur by a first-order transition, but is a gradual rotation.

The spin reorientations which occur in many of the rare-earth orthoferrites have been investigated by various techniques.¹⁻⁵ Mössbauer measurements recently performed^{4,5} on ErFeO₃ showed that spin reorientation proceeds by a gradual and uniform spin rotation and not by a first-order transition (discontinuous 90° spin flip) occurring in different regions of the sample at different temperatures.

In the present communication we confirm the Mössbauer results by directly monitoring the orientation of the spins as they change their direction as a function of temperature. This technique is based upon the fact that the neutron-scattering cross section from a magnetic reflection is proportional to the quantity $\sin^2\phi$, where ϕ is the angle between the scattering vector and a vector parallel to the spin direction.⁶ If a reflection is chosen whose scattering vector is parallel to the reorientation plane and

if the spin reorients continuously with temperature, the neutron intensity may go through a maximum or a minimum depending on the angle and sense of the rotation. On the other hand, if the rotation is a discontinuous spin flip (but at different temperatures in different parts of the crystal), then the neutron intensity will change monotonically. It is also necessary that all spins rotate in the same direction (clockwise or counterclockwise). Otherwise the maximum or minimum may be averaged out. In the case of the rare-earth orthoferrites, a magnetic field is used to act on the weak ferromagnetic moment associated with the dominant antiferromagnetism in order to satisfy this condition.

We have applied this technique to a single crystal of ErFeO₃. The crystal structure of this compound belongs to the orthorhombic space group *Pbnm*.⁷ In the reorientation range ~90-100°K, upon heat-